# Chapter 8

## Field emission from well-aligned carbon nanotips

### 8.1 Introduction

In this study, new carbon nanomaterials are developed in field emission. Well-aligned carbon nanotips were grown on the platinum (Pt) films in the chemical vapor deposition system. Carbon nano-tips with a high-aspect-ratio were directly grown on Pt films. Carbon nanotips grew up to 5.4 μm length and 64 nm diameter under a –120V bias. Compared to the hollow structure of carbon nanotubes, transmission electron microscopy (TEM) images indicate its solid body, which is made of graphite. Carbon nanotips possess good field emission characteristics, that is, a turn-on field of 1.5 V/μm and 761 $\mu A/cm^2$ under 2.2 V/μm. The Pt films provide a good conduction path for electron transport from the cathode to the emission site and do not act as catalysts.

Basically, carbon nanotubes were synthesized with metal catalysts such as Fe, Co, Ni, and others [1-3]. These metal catalysts play a key role in the deposition. However, a Pt film which is highly chemically inert provides only a good conduction path for electron transport from the cathode to the emission sites instead of catalysts. Therefore, the intrinsic properties of carbon nanotips are different from carbon nanotubes.

In addition, well-aligned with high-aspect-ratio nanotips are also directly synthesized in a 4 μm gated device structure by using $CH_4/CO_2$ gaseous mixture. The growth rate of nanotips is higher in highly carbon-concentrated $CH_4/CO_2$ gas mixture than in conventional mixtures of hydrocarbons diluted in hydrogen.

**Part A: Field emission of well-aligned carbon nanotips in diode structure**

**8.2A. Experiment**

5 nm Ti (the improvement of adhesion between Si and Pt) and 20 nm Pt films were precoated sequentially on Si by using electron beam evaporation. The reactive gas mixture was $CH_4/H_2$ with a flow rate of 10/10 sccm. The applied microwave power and the pressure during the growth of carbon nanotips were 400 W and 15 torr, respectively. An optical pyrometer was used to monitor the substrate temperature, that was maintained at about 700 ºC. The growth time was 45 minutes, but nanotips grown on Si under a –120V bias only lasted for 30 minutes.

**8.3A. Results and Discussion**

**(I) Scanning electron microscope (SEM)**

It is considered that the carbon active species in the plasma are accelerated to the substrate by the negative bias to form $sp^2$ and non-crystalline clusters in the nucleation period. Some clusters are then transformed into $sp^3$ clusters through the collision of carbon species in the growth period. Meanwhile, the accelerated active hydrogen radicals will remove the other $sp^2$ clusters with lower active energy. In this

situation, the competition between etching and deposition is repeated. Nevertheless, biasing the samples can cause their rate of deposition to exceed the rate of etching. Many reports have presented the method to enhance the nucleation density of diamond by applying negative bias [4-6]. This study focuses mainly on determining the optimum negative bias to synthesize the carbon nanotips. Figures 8.1 and 8.2 present the scanning electron microscope (SEM) pictures of carbon nanotips grown under various biases and substrates. The photograph on the right of each figure is the enlarged image. Fig.8.1 (a) displays that there only a low density of tiny nanotips can be grown under –80V. This also implies that samples grown under a bias less negative than –80V cause little carbon materials to be deposited on the Pt films. Increasing the bias to –120V, it generates the high-density carbon nanotips. Fig. 8.2 (a) shows these well-aligned carbon nanotips grown upward to 5.4 μm length and 64 nm in diameter under –120V. Sharper nanotips have a higher-aspect-ratio, indicating good characteristics for field emission. Fig. 8.1(b), however, indicates that tips will grow to a sub-micrometer diameter under a higher bias (more negatives than –120V), revealing that bias can enhance the growth of carbon nanotips on Pt films. Hence, the optimal bias for growing carbon nanotips on Pt films is –120V.

(a)

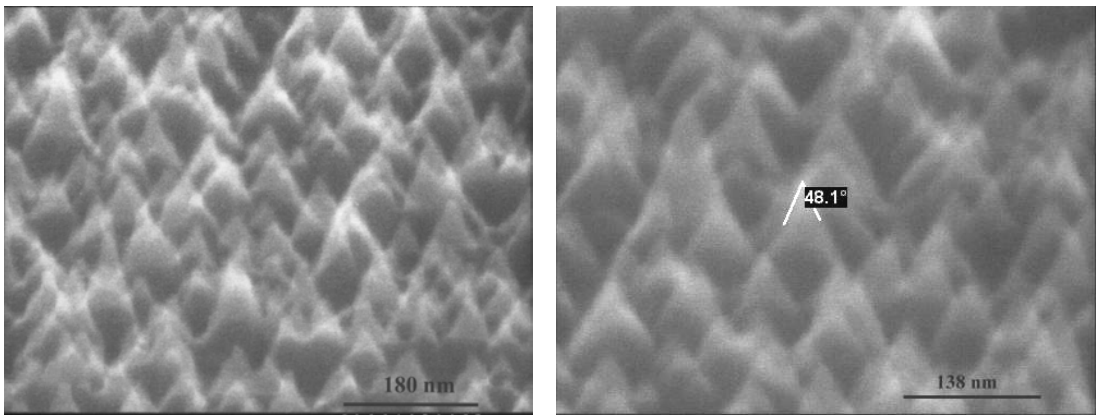


(b)

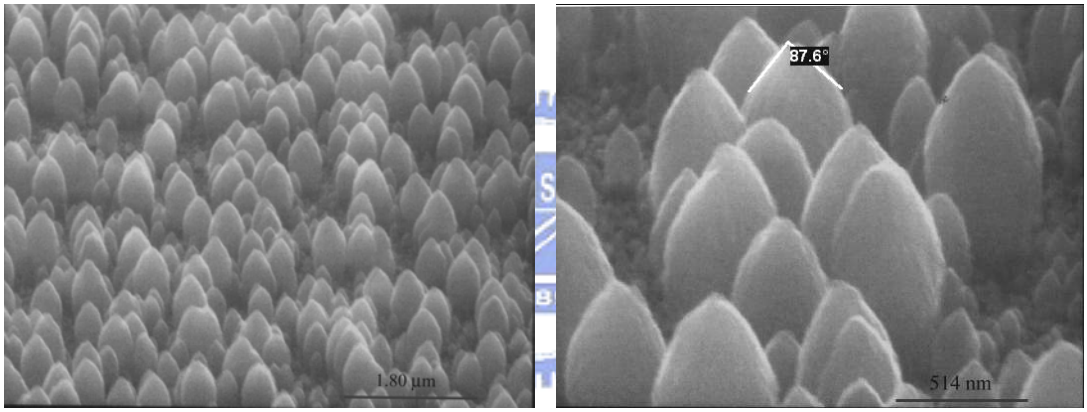


Fig. 8.1 SEM photographs of carbon nanotips grown on Pt under (a)–80V and (b)–150V.

(a)

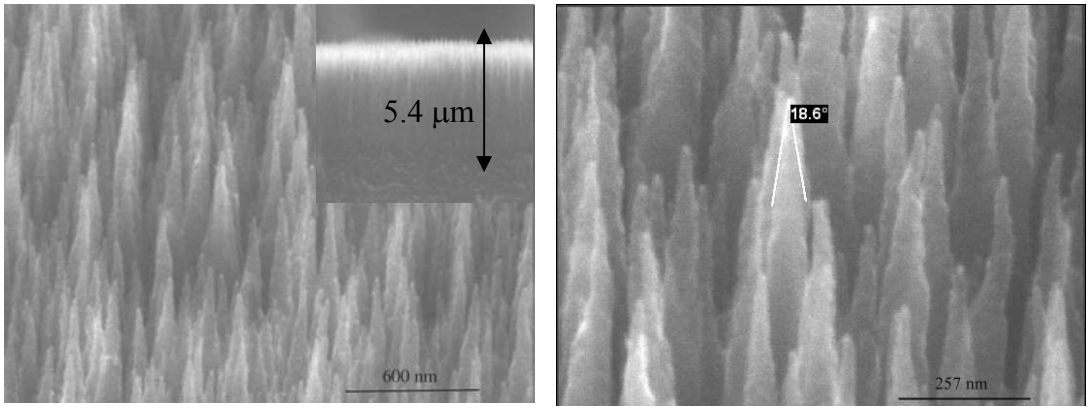


(b)

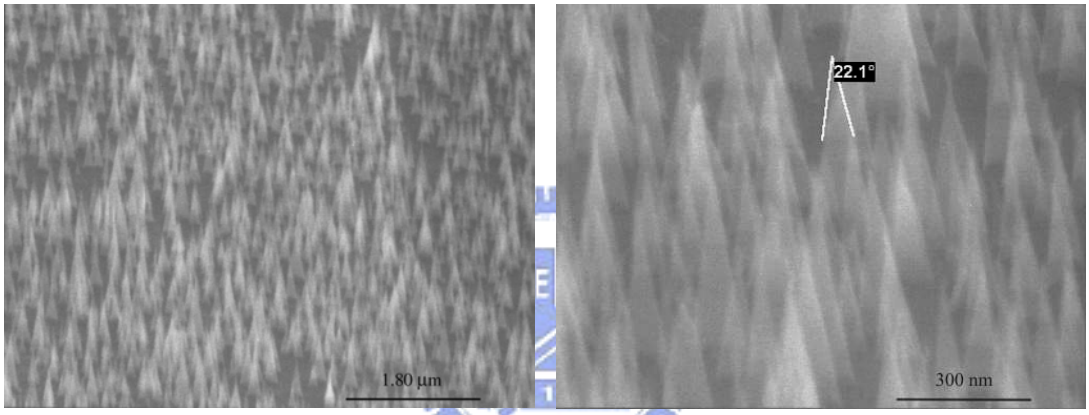


Fig. 8.2. SEM photographs of carbon nanotips grown under –120V on (a) Pt and (b) Si.

Figure 8.2 (b) also shows good results of carbon nanotips grown on Si under –120V, but the deposition time is shorter than those grown on Pt films. This is due to the fact that it is easier to form carbon materials on Si than on Pt [7].

**(II) Transmission electron microscope (TEM)**

Figure 8.3 (a) displays the TEM images of an end section of an individual nanotip grown under –120V. Unlike hollow carbon nanotubes, carbon nanotips are solid. The main feature of note is the tip's somewhat irregular shape, with one primary protrusion. The diffraction pattern (DP) indicates that the end section is graphite. Moreover, Fig. 8.3 (b) displays the lateral section of the same tip, showing well-organized microcrystalline graphite section. The DP of Fig. 8.3 (b) also confirms the existence of well-organized microcrystalline graphite, proving that the carbon nanotips are made of graphite. Besides, through high-resolution TEM images, the calculated inter-plane spacing are 0.34 nm, directly confirming the graphite structures.

**(III) Raman spectra**

Figure 8.4 exhibits the Raman spectra of carbon nanotips grown under various bias and substrates. All of them have two sharp peaks located on about 1345 $cm^{-1}$ and 1580 $cm^{-1}$, respectively.

(a)

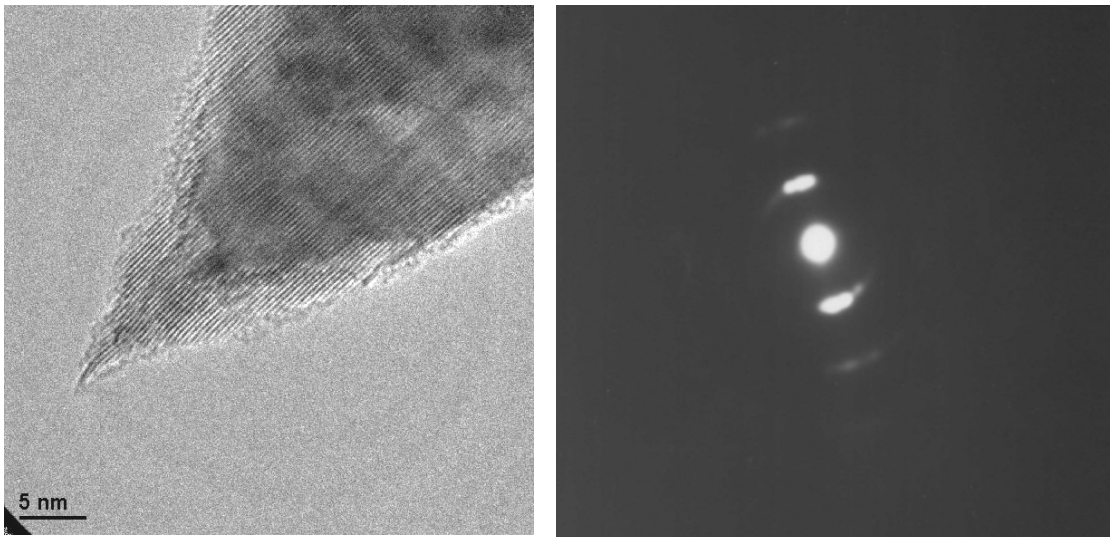


(b)

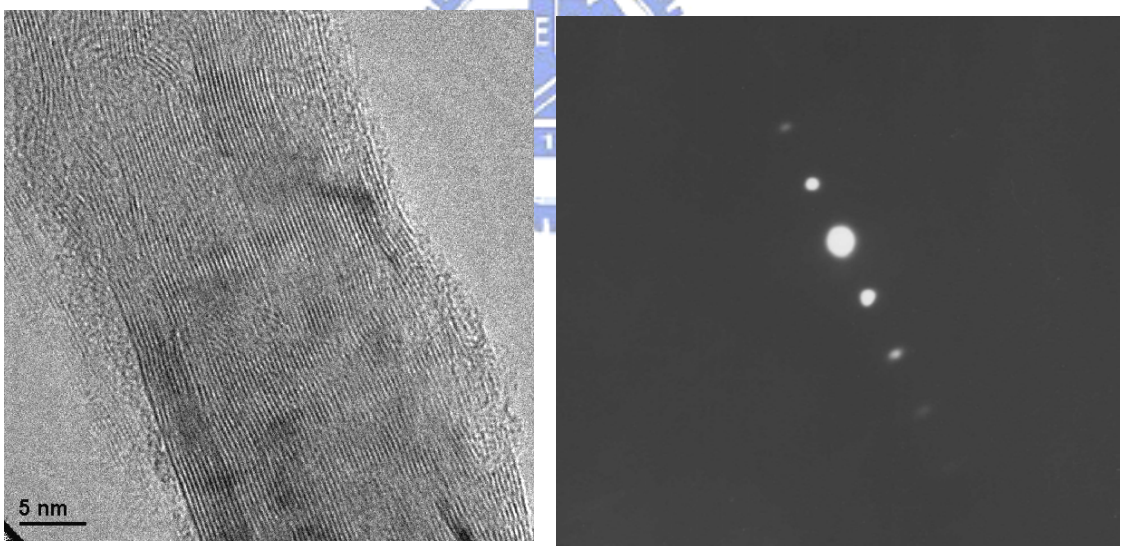


Fig. 8.3. TEM images and diffraction pattern of (a) the end section and (b) lateral section of an individual tip.

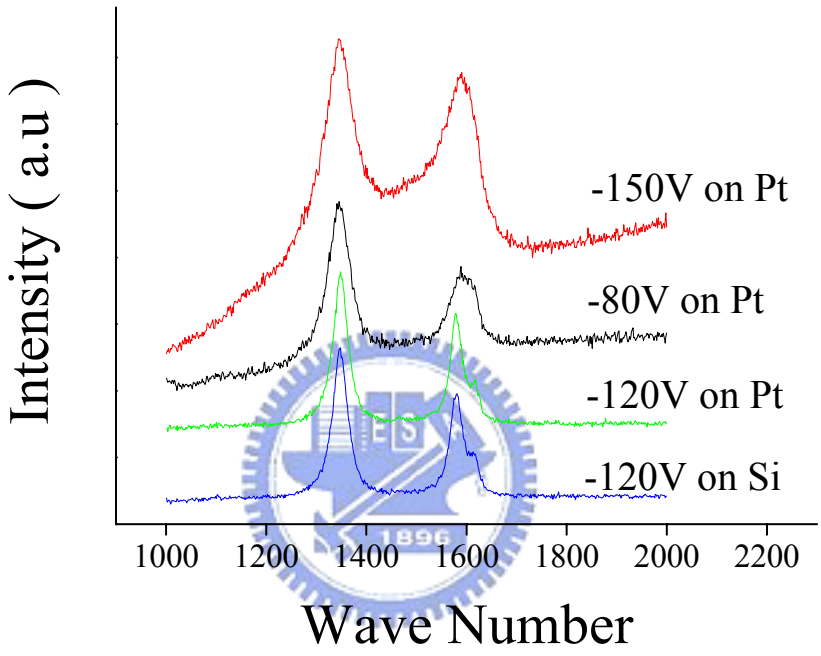


Fig. 8.4. Raman spectra of carbon nanotips grown under various biases and substrates.

The first-order Raman spectrum of aligned carbon nanotips shows strong sharp peaks at 1581 $cm^{-1}$ (G line), which is the high-frequency $E_{2g}$ first-order mode and 1350 $cm^{-1}$ (roughly corresponding to the D-line associated with disorder-allowed zone-edge modes of graphite). The peaks imply that the nanotips are characteristic of microcrystalline graphite. The relative intensities of the two peaks depend on the type of graphitic material. Normally, the intensity of the 1350$cm^{-1}$ peak increases (i) with an increase in the amount of unorganized carbon in the samples and (ii) with a decrease in the graphite crystal size [8].

The most conspicuous feature of carbon nanotips (grown under –120V) is that their Raman spectra show an additional weak peak at about 1618 $cm^{-1}$ (D' line). The origin of the D and D' lines in other forms of carbon materials has been explained as disorder-induced features, caused by the finite particle size effect or lattice distortion [9-11]. Besides, a sample grown under –120 V with a narrow bandwidth of the G-line and the D-line has well-organized carbon. The previous TEM image clearly displays the existence of well-organized graphite in the sample.

**(IV) I-V characterization**

The field emission tests are performed on a diode structure, in which the carbon nanotips are separated from the anode, indium-tin-oxide glass, using 500 μm glass as spacers. The voltage-current ( *I-V* ) properties are measured and analyzed through the

Fowler-Nordheim (FN) model, via the ln ( $I/V^2$ ) VS. $I/V$ plot. Fig. 8.5 characterizes carbon nanotips grown under –120V on Si and Pt. The current densities at 2.2 V/μm of nanotips under –120V grown on Pt and Si are 761 and 617 μA/cm$^2$, respectively. The threshold voltage ( $V_T$ ) is defined as the intersection of the slope of F-N plots with abscissa. According to the F-N analysis, the emission behavior of the sample grown on the Pt films is better than that grown on Si (lower turn-on field = 1.5 V/μm). It is attributed to the presence of Pt layers, which provide a good conduction path for electron transport from the cathode to the emission sites [12].

(a)

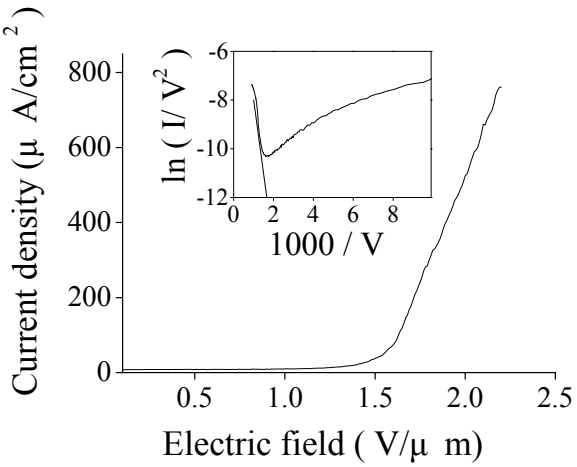


(b)

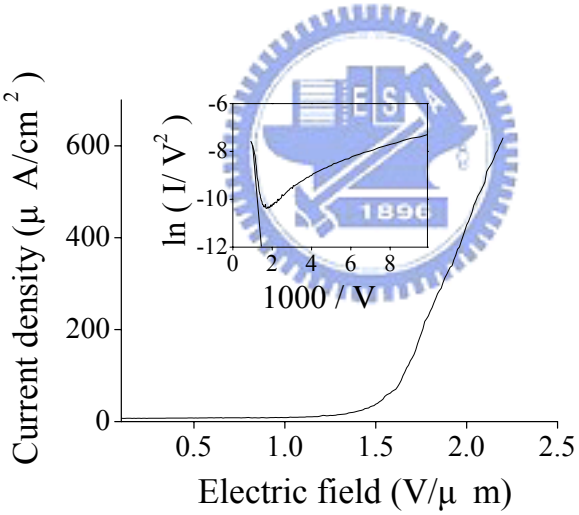


Fig. 8.5. The current density versus electric field and F-N plot of carbon nanotips grown under –120V on (a) Pt and (b) Si.

**Part B: Field emission of well-aligned carbon nanotips in gated structure**

**8.2B. Experiment**

A Pt-gated device structure with 50 x 50 circles was initially fabricated by semiconductor process technology. Starting substrates were mirror-polish n-type, (100) oriented wafers. The width and the depth of each circle were 4 μm and 7000Å, respectively. After the gated device structure was generated, specimens were put in the bias-assisted microwave plasma chemical vapor deposition system to deposit carbon nanotips. Reactive gaseous mixture of $CH_4$-$CO_2$ was used in deposition. The flow rates of $CH_4/CO_2$ and the deposition time remained constant at 30/30 sccm and 15 minutes, respectively. During deposition, the Si substrate was subjected to various negative bias voltages. The following table lists the experimental conditions.

**Table 8.1 Deposition conditions of carbon nanotips.**

| Sample | Flow rate $CH_4/CO_2$ sccm | Negative Bias (V) | Deposition time (Min) |
|---|---|---|---|
| A | 30/30 | 120 | 15 |
| B | 30/30 | 130 | 15 |
| C | 30/30 | 150 | 15 |
| D | 30/30 | 180 | 15 |

Total pressure = 15 torr
Microwave power = 300 W Substrate temp. (℃) = ~750

**8.3B. Results and Discussion**

**(I) Scanning electron microscope (SEM)**

Figure 8.6 shows SEM photographs of carbon nanotips grown under different biases. Each picture is only one of the 50 x 50 circles on the device. On the right side

of every picture is an enlarged image. The SEM images indicate that carbon nanotips can be uniformly grown only inside the Pt-gated device structure in the absence of amorphous carbon (a-C) on the Pt-gated surface. The selective area deposition of nanotips is attributed to the following two reasons. One is that carbon materials are more easily grown on silicon than on the Pt-gated layer because Pt is a highly chemically inert material that does not nucleate carbon materials on an unscratched Pt surface [12-13]. The other is that electrical field is concentrated on the silicon substrate surface because the n-type silicon conducts electrons, but electrons can not pass through silicon dioxide (dielectric layer) within a Pt-gated layer. Consequently, the local deposition biased effects are all within the silicon substrate. However, increasing the deposition time causes some a-C to form on the Pt-gated surface.

Figures 8.6(a) ~ (c) reveal that applying a bias can enhance the growth of carbon nanotips in $CH_4/CO_2$ gas mixture. Thus, the higher bias drastically enhances the growth of carbon nanotips. The bias-assisted effect is also valid for the hydrocarbon diluted in hydrogen [14]. However, samples grown under a bias more negative than -130V cause the height of the tips to exceed that of the Pt-gate. In this situation, the gated device structure becomes a diode structure. By contrast, a bias less negative than -130V only leads to tiny tips inside the hole. In addition, all the tips grow upward under biased conditions. The tip angle of the nanotips decreases as the bias increases.

( a )

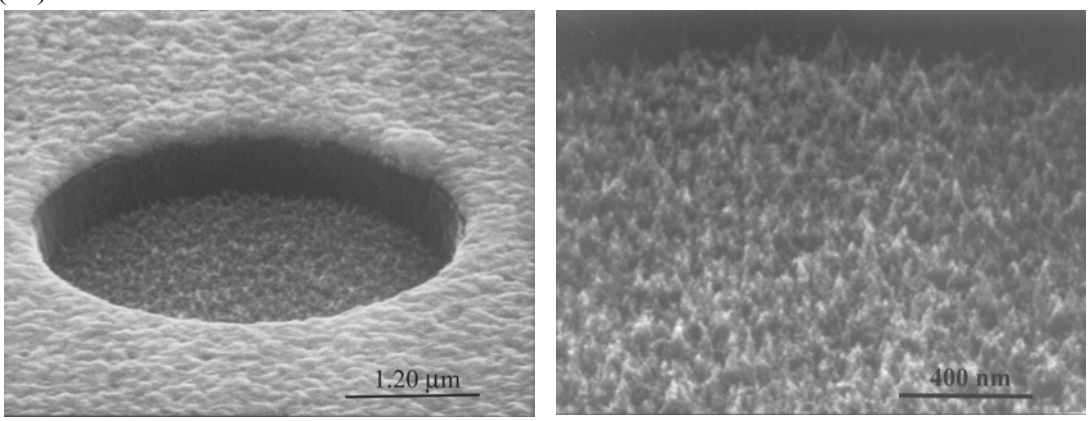


( b )

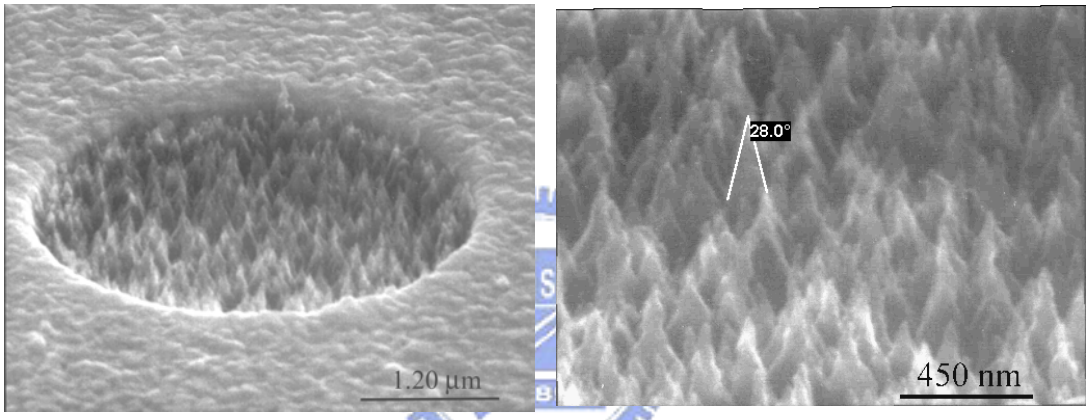


( c )

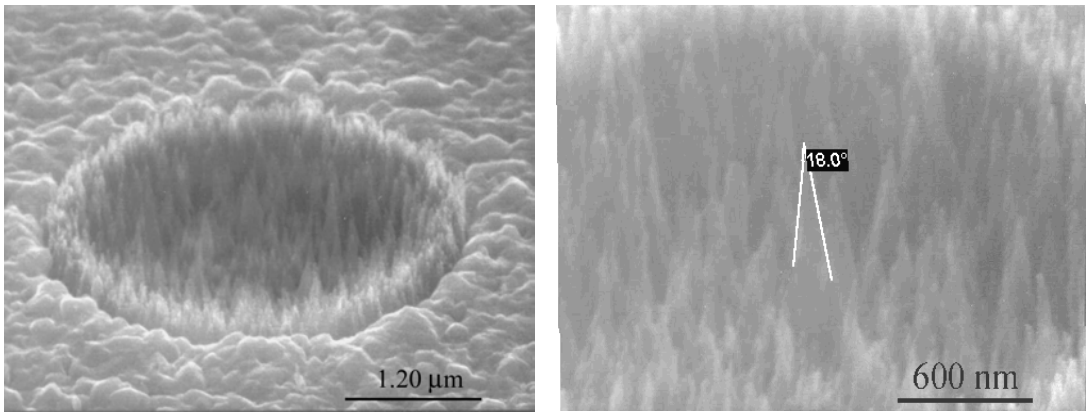


Fig. 8.6. SEM photographs of nanotips grown under (a) -100V, (b) -130V and (c) -150V

In other words, a higher bias generates higher density, sharper and higher-aspect-ratio nanotips. $CH_4/CO_2$ can promote the growth rate over that with conventional gas mixtures (hydrocarbons diluted in hydrogen, for example, $CH_4/H_2$) [15] because of the high carbon concentration in the $CH_4/CO_2$ gas mixture.

**(II) Transmission electron microscope (TEM)**

Figure 8.7 (a) displays the TEM images of an end section of an individual nanotip. The main feature of note is the tip's somewhat irregular shape, with one primary protrusion. The Fourier filtering transformation (FFT) indicates that the end section is amorphous carbon. Moreover, Fig. 8.7 (b) displays the lateral section of the same tip. It shows microcrystalline graphite on the lateral section. The FFT of Fig. 8.7 (b) also proves the existence of the microcrystalline graphite.

**(III) Raman spectra**

Figure 8.8 presents Raman spectra of tips grown under various applied biases. The spectra do not obviously differ. All of them have two sharp peaks located on about 1355 $cm^{-1}$ and 1582 $cm^{-1}$, respectively. The peaks imply that the nanotips are characteristic of microcrystalline graphite. The Raman spectra of amorphous carbon can be decomposed into two features located approximately at 1550$cm^{-1}$ (corresponding to the G-line associated with the optically allowed $E_{2g}$ zone center mode of crystalline graphite) and 1350 $cm^{-1}$ (roughly corresponding to the D-line

associated with disorder-allowed zone-edge modes of graphite). The positions, widths, and relative intensities of these two peaks are found to vary systematically with deposition conditions and tips' properties [16-17]. The intensity of these two peaks is the same indicating that the samples contain much amorphous carbon.

**(IV) I-V characterization**

Figure 8.9 displays the electron-emitting characteristic of the nanotips on gated device structure. The field emission properties are measured by using a triode technique. An anode plate, an ITO Glass, is placed above the Pt gate and biased to +800 V. A 100 μm slide glass is used for the spacer. The anode current ($I_A$) is then measured as a function of gate-to-cathode bias voltage in a vacuum of $1\times10^{-6}$ torr. The gate-to-cathode voltage ($V_{gc}$) is varied from 0 to 50 V. The field emission current ($I_a$) of nanotips on the gated device structure is about 154 μA (at a gate-to -cathode voltage of $V_{gc}$= 50V). Therefore, the higher emission current of the nanotips results from the following causes. (I) short gate-tips spacing, (II) small gate aperture, and (III) the high-aspect-ratio of the nanotips.

( a )

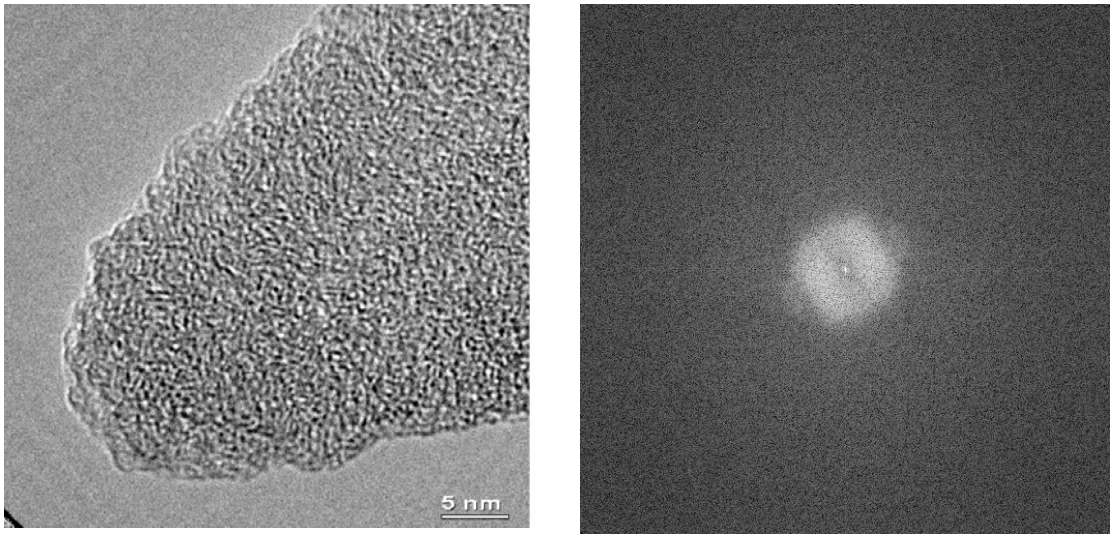


( b )

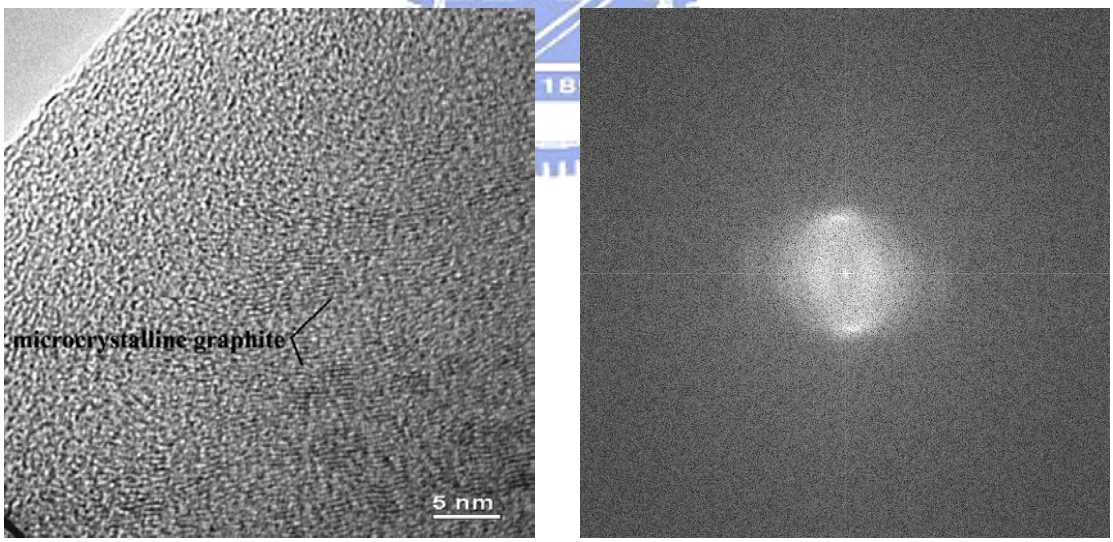


Fig. 8.7. TEM images and Fourier filtering transformation (FFT) of (a) the end section and (b) lateral section of an individual tip.

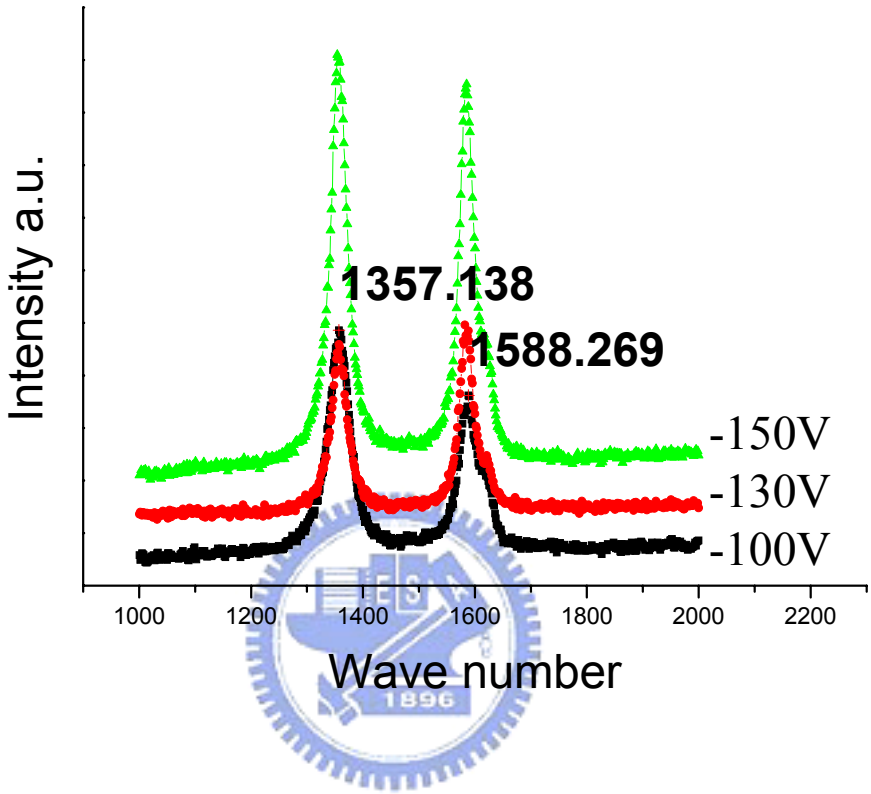


Fig. 8.8. Raman spectra of nanotips growing under different applied biases

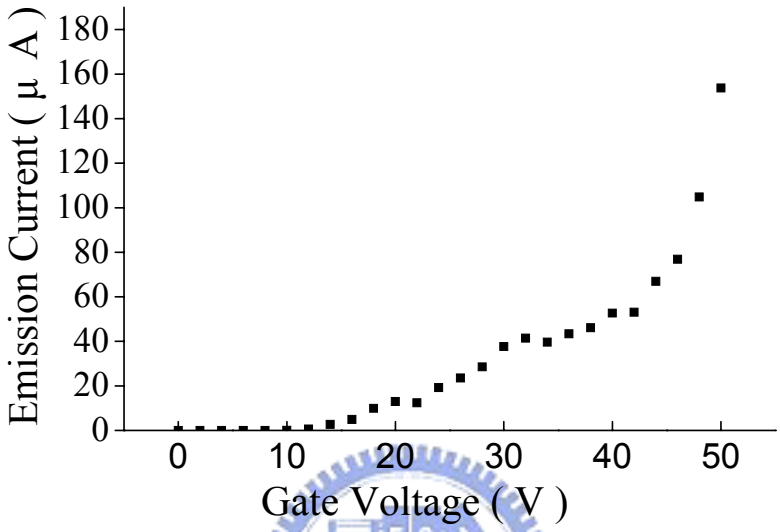


Fig. 8.9 The emission current versus the gate voltage of nanotips on a gated device structure.

## 8.4 Conclusion

In this chapter, carbon nanotips are synthesized by using microwave plasma chemical vapor deposition system. Major results are summarized as follows:

1. Carbon nanotips grew up to 5.4 μm length and 64 nm in diameter under applying a –120 V bias during deposition.
2. Compared to the hollow body of carbon nanotubes, TEM images indicate carbon nanotips show solid structure, which is made of graphite.
3. With high aspect ratio property, carbon nanotips possess good field emission characteristics, that is a turn-on filed of 1.5 V/μm and 761 μ A/cm$^2$ under 2.2 V/μm.
4. Instead of catalyst role, the Pt films provide a good conduction path for electron transport from the cathode to the emission sites.
5. The file emission current of carbon nanotips grown on the gated structured is 154μ A (at a gate–to-cathode of $V_{gc}$=50 V). This results from the following reasons: (I) short gate-tips spacing; (ii) small gate aperture, and (iii) the high aspect ratio of carbon nanotips.

## 8.5 Reference


1. Chris Bower, Otto Zhou, Wei Zhu, D.J.Werder, and Sungho Jin. Appl. Phys. Lett, 77, 2767 (2000).

2. J.Kim, K.No, and C.J.Lee, J. Appl. Phys. 90, 2591 (2001).

3. J.I.Sohn, S.Lee, Y.H.Song, S.Y.Choi,K.L.Cho, and K.S.Nam, Appl.Phys.Lett, 78, 901 (2001).

4. S.Yugo, T.Kanai, T.Kimura and T.Muto, Appl. Phys. Lett, 58, 1036 (1991).

5. Huang, J.T.; Yeh, W.Y.; Hwang, J.; Chang, H. Thin Solid Films 315, 35 (1998).

6. Stöckel, R.; Janischowsky, K.; Rohmfeld, S.; Ristein, J.; Hundhausen, M.; Ley, L. Diam.Relat.Mat 5, 321 (1996).

7. T. Tachibana, Y. Yokota, K. Hayashi, K. Miyata, K. Kobashi and Y. Shintani Diam. Relat. Mater., 9, 251 (2000).

8. F. Tuinstra and J.L.Koenig, J.Chem.Phys. 53, 1126 (1970).

9. G. Vitali, M. Rossi, M. L. Terranova, and V. Sessa, J. Appl. Phys. 77, 4307 (1995).

10. D. G. McCulloch, S. Prawer, and A. Hoffman, Phys. Rev. B 50, 5905 (1994).

11. V. Barbarossa, F. Galluzzi, R. Tomaciello, and A. Zanobi, Chem. Phys. Lett. 185, 53 (1991).

12. J.S.Lee; K.S.Liu and I.N.Lin, Appl.Phys.Lett. 71, 554 (1997).

13. D.N.Belton and J.Schmeig. J.Appl.Phys. 69, 3032 (1991).

14. S. Yugo, T. Kanai, T. Kimura, and T. Muto, Appl. Phys.Lett, 58, 1036 (1991).

15. Chia-Fu Chen, Hui-chen Hsieh, Diamond Relat. Mater. 9, 1257 (2000).

16. M.A. Tamor and W.C. Vassell, J.Appl.Phys 76 (6), 3823 (1996).

17. J. Wagner, M. Ramsteiner, Ch. Wild, and P.Koidl, Phys. Rev. B 40 1817 (1989).